# Neural Impedance Adaption for Assistive Human-Robot Interaction

Hamed N. Rahimi [a], Ian Howard [b], and Lei Cui [c]

*Department of Mechanical Engineering, Curtin University, Perth, 6102, Western Australia*

a. Email: hamed.rahiminohooji@postgrad.curtin.edu.au; Tell: (61) 8 9266 7591; Orcid: 0000-0001-9429-7164
b. Email: i.howard@curtin.edu.au; Orcid: 0000-0003-3999-9184
c. Email: lei.cui@curtin.edu.au; Orcid: 0000-0003-2283-5079

**Abstract.**

The problem of assistive human-robot interaction (HRI) with unknown impedance parameters is nontrivial and interesting. This problem becomes even more challenging if unknown reference trajectory and uncertain robot dynamics are involved. This study investigates an intelligence impedance adaption control scheme to assist human interaction with an unknown robot system. An algorithm is proposed to facilitate assistive HRI by optimizing the overall human–robot interaction performance. Neural networks (NN) and backpropagation are employed to tackle the optimization problem, based on an online adaption of impedance parameters. The tuned impedance model is integrated into the design of the neuroadaptive controller. The controller is modified by utilizing the barrier Lyapunov function technique to increase the safety, and to improve functionality of the NN during the system operation. The obtained controller can learn the robot dynamics online while coping with both the problems of trajectory-following and impedance model-following. Stability and uniform boundedness of the closed-loop system are verified through Lyapunov direct analysis. The effectiveness of the proposed control design is validated by theoretical analysis and numerical simulation.

**Keywords.** Impedance adaption; Neuro-adaptive control; Assistive human-robot interaction; Backpropagation; Barrier Lyapunov function.

## 1. Introduction

Impedance control that aims to control the dynamic behavior has recently gained increasing importance as the focus of robotic applications shifts from industrial robots to social ones. In fact, as daily applications such as elderly care, health care, and education make their way into the robotic research, the control of motion/force became inadequate to handle the interaction task. Instead, impedance control and specifically adaptive impedance control that aims to provide safety and to reduce dependency on precise knowledge of the robot dynamics has undergone rapid progress over the past decade.

### *1.1. Related works and motivation*

In several studies on impedance control, a desired fixed passive impedance model was prescribed, and then efforts were focused on some challenges like handling the uncertainties. Works which fall under this framework typically have employed learning impedance control [1], or adaptive impedance control [2]. However, assuming fixed impedance models is no

longer sufficient to describe some applications like explosive movement [3], or HRI [4]. Accordingly, employing variable impedance control must be considered [3, 4]. Nevertheless, to achieve improved interaction performance, it appears more effective to tune impedance parameters to provide optimal impedance characteristics, which are required for such important applications like HRI. In [5] adaptive impedance motion learning for physical HRI was presented. In this study, robot anticipated the partner's intentions to adapt the motion by task learning. Optimal impedance adaptation was studied for constrained motion HRI in [6]. Continuous critic learning was utilized for interaction control then, the desired impedance was obtained to be used as an optimal realization for satisfying control objective.

In the development of HRI with unknown impedance models, methods like impedance learning or impedance adaption have been investigated. Starting from the 1984 seminal works by Arimoto, Kawamura, and Miyazaki [7, 8] several researchers employed iterative learning control to obtain impedance parameters in designing robot controls . This method was based on the notion that improvement of performance can be achieved by repeating a task and learning from previous executions. In [9] a two-loop impedance learning control framework was studied to solve the robot-environment interaction problem. An adaptive control was utilized for the inner-loop position control. Desired impedance model were obtained using the gradient-following and betterment schemes via minimizing a cost function is minimized. Surveys on iterative learning control with the brief categorization of the method can be found in [10-12]. However, as this method makes the robot repeat operations to learn the desired impedance parameters, it may cause inconvenience in several situations, specifically when online or complex tasks are required.

Compared to iterative impedance learning methods, in the impedance adaptation method, impedance parameters can be tuned without requiring the operation to be repeated [13]. However, developing an adaptive scheme is a challenging issue. In this method, to adjust the impedance parameters, several concerns can be raised regarding the improvement of system performance e.g. the input torque [14], the stability [15], minimizing a cost function [16], and developing assistive HRI [17, 18]. Moreover, many techniques have been employed to solve the problem of finding impedance parameters. Moreover, many techniques have been employed to solve the problem of finding impedance parameters. Sam Ge et al. used adaptive dynamic programming for impedance adaptation in an optimal robot–environment interaction [13]. Yanan Li et al. employed approximate dynamic programming to find impedance parameters in the shared control of human and robot [19]. Modares et al. employed reinforcement learning to obtain optimized assistive HRI in [18]. Game theory was utilized to solve the problem of impedance parameters finding in continuous role adaptation for human–robot shared control [20], and adaptive optimal control for coordination in physical HRI [21]. This method was also combined with policy iteration to obtain impedance parameters for human–robot coordination in [22].

The aim of control design in this paper is to propose a stable, intelligent assistive HRI scheme with unknown robot dynamics and impedance behavior. The method is based on neural adaptive impedance control, and future backpropagation methods to find impedance parameters. The control structure consists of two control loops, namely an inner-loop and an outer-loop. The former is designed to provide a constrained torque controller to make unknown robot dynamics respond like a prescribed robot impedance model without knowing the reference trajectory. The latter is exploited to afford assistive HRI by adjustment of impedance parameters.

### *1.2. Contributions and structure of the paper*

The contributions of this paper can be highlighted as follows.

1. A neural adaptive impedance control is developed for an uncertain robotic system with unknown impedance model, by introducing a new inner-loop, outer-loop control structure.

2. An Inner-loop controller is designed to make an unknown robot behave like an impedance model with unknown reference trajectory. The presented controller does not require adapting robot impedance model parameters in this control loop. In addition, safe and constrained control is designed by utilizing the advantages of the barrier Lyapunov functions.

3. An outer-loop controller is designed to tune unknown impedance parameters such that assistive HRI is directed. To do this, NN and the backpropagation method are utilized to minimize the cost function in terms of the trajectory-following error and the interaction force.

The rest of the paper is organized as follows. In the next section, the dynamics of the robot and human limb model are described, and control objective of the paper is discussed. Section 3 presents the HRI control structure; first, the overall structure of the developed approach is briefly discussed then, the inner-loop and outer-loop control designs are detailed. Simulation results are presented in Section 4, and finally Section 5 concludes this paper.

**Notations:**

Throughout this paper, $\mathbf{R}$ and $\mathbf{R}^+$ are used to denote the sets of real numbers and non-negative real numbers, respectively. $\tilde{(\bullet)}=(\bullet^*)-(\hat{\bullet})$, with $(\hat{\bullet})$, and $(\bullet^*)$ represent estimated, and optimal values of $(\bullet)$, respectively. Vertical bars $\|\bullet\|$ denote the Euclidean norm for vectors or the Frobenius norm for matrices, $\lambda_{\min}(\bullet)$ and $\lambda_{\max}(\bullet)$ represent the smallest and largest eigenvalues of a square matrix $(\bullet)$, respectively.

## 2. System overview and preliminaries

### *2.1. System description*

A system where a robotic arm physically interacts with a human is studied in this paper. Consider the dynamic model of robot manipulator in the Cartesian space as [23]:

$$\boldsymbol{M}(\boldsymbol{q})\ddot{\boldsymbol{x}}+\boldsymbol{C}(\boldsymbol{q},\dot{\boldsymbol{q}})\dot{\boldsymbol{x}}+\boldsymbol{G}(\boldsymbol{q})=\boldsymbol{\tau}+\boldsymbol{f}_{\boldsymbol{H}}, \tag{1}$$

where $\boldsymbol{M}=\boldsymbol{J}^{-T}\bar{\boldsymbol{M}}\boldsymbol{J}^{-1}$ , $\boldsymbol{C}=\boldsymbol{J}^{-T}\left(\bar{\boldsymbol{C}}-\bar{\boldsymbol{M}}\boldsymbol{J}^{-1}\dot{\boldsymbol{J}}\right)\boldsymbol{J}^{-1}$ ,$\boldsymbol{G}=\boldsymbol{J}^{-T}\bar{\boldsymbol{G}}$, $\boldsymbol{\tau}=\boldsymbol{J}^{-T}\bar{\boldsymbol{\tau}}$, $\boldsymbol{q}\in\mathbf{R}^{\boldsymbol{n}}$ is the generalized joint coordinate vector with $\boldsymbol{n}$ number of joints, $\boldsymbol{x}\in\mathbf{R}^{\boldsymbol{n}}$ is the end-effector Cartesian position, $\boldsymbol{J}\in\mathbf{R}^{\boldsymbol{n}\times\boldsymbol{n}}$ is the Jacobian matrix, $\bar{\boldsymbol{M}}\in\mathbf{R}^{\boldsymbol{n}\times\boldsymbol{n}}$ denotes the mass (inertia) matrix, $\bar{\boldsymbol{C}}\in\mathbf{R}^{\boldsymbol{n}\times\boldsymbol{n}}$ represents the centrifugal and Coriolis forces matrix, $\bar{\boldsymbol{G}}(\boldsymbol{q})\in\mathbf{R}^{\boldsymbol{n}}$ is the vector of gravitational forces/torques; $\bar{\boldsymbol{\tau}}\in\mathbf{R}^{\boldsymbol{n}}$ is the vector of generalized continuous torques acting at the joints, and $\boldsymbol{f}_{\boldsymbol{H}}$ is the the interaction force between the human and robot. Note that the robot manipulator dynamics in (1) are assumed to be unknown.

**Property 1** [24]: The inertia matrix $\boldsymbol{M}$ is symmetric and positive definite. Also, the matrix $2\boldsymbol{C}-\dot{\boldsymbol{M}}$ is a skew symmetric matrix if $\bar{\boldsymbol{C}}$ is in the Christoffel form, i.e. $\Theta^T\left(2\boldsymbol{C}-\dot{\boldsymbol{M}}\right)\Theta=0$, $\forall\Theta\in\mathbf{R}^n$.

### *2.2. Problem statement*

The main objective of control architecture in this paper is to design the force $\boldsymbol{\tau}$ in (1) to let the robot move along a desired trajectory $\boldsymbol{x}_d$ while the interaction force $\boldsymbol{f}_H$ is minimized, and the robot dynamics (1) respond like the following target impedance model,

$$\boldsymbol{M}_r\ddot{\boldsymbol{x}}_b+\boldsymbol{B}_r\dot{\boldsymbol{x}}_b+\boldsymbol{K}_r\boldsymbol{x}_b=\boldsymbol{f}_H, \tag{2}$$

where $\boldsymbol{x}_b=\boldsymbol{x}_m-\boldsymbol{x}_d$ with $\boldsymbol{x}_m$ being the unknown reference trajectory; $\boldsymbol{M}_r$, $\boldsymbol{B}_r$, and $\boldsymbol{K}_r$ are unknown desired inertia, damping, and stiffness parameter matrices, respectively. To satisfy the control objective design, we define the model-following error variable to be $\boldsymbol{e}_1=\boldsymbol{x}_m-\boldsymbol{x}$, and the trajectory-following error to be $\boldsymbol{e}_2=\boldsymbol{x}_m-\boldsymbol{x}_d=\boldsymbol{x}_b$ which is to be minimized. Also, an algorithm is designed to minimize $\boldsymbol{f}_H$ by properly modifying the impedance model parameters.

**Assumption 1.** The desired trajectory $\boldsymbol{x}_d$, and the reference trajectory $\boldsymbol{x}_m$ are bounded.

**Remark 1.** The selection of impedance model parameters $\boldsymbol{M}_r$, $\boldsymbol{B}_r$, and $\boldsymbol{K}_r$ depends on different applications. In particular, as the reference model (2) defines a desired dynamic relationship between the model-following error and the interaction force, choosing a passive impedance model is too conservative [13]. This paper aims to find the critical impedance parameters by optimizing the overall HRI performance. Accordingly, the assistive human-robot interaction can be conducted by updating the impedance parameters.

**Remark 2.** The relation between $\boldsymbol{e}_1$ and $\boldsymbol{e}_2$ can be established as $\boldsymbol{e}_2=\boldsymbol{e}_1+\boldsymbol{x}-\boldsymbol{x}_d$. Accordingly, in view of Assumption 1, it holds that if $\boldsymbol{e}_1\in\ell_\infty$, then $\boldsymbol{x}$ is bounded, and accordingly $\boldsymbol{e}_2\in\ell_\infty$ can be concluded. Thus, the key in designing the tracking control scheme is to ensure the boundedness of $\boldsymbol{e}_1$ which is addressed in the inner loop control design.

### *2.3. Human limb model*

Dynamics of a human limb, in general, can be described by,

$$\boldsymbol{M}_H\ddot{\boldsymbol{x}}+\boldsymbol{C}_H\dot{\boldsymbol{x}}+\boldsymbol{G}_H\left(\boldsymbol{x}-\boldsymbol{x}_d\right)=-\boldsymbol{f}_H, \tag{3}$$

which includes mass-damper-spring property, where $\boldsymbol{M}_H$, $\boldsymbol{C}_H$, $\boldsymbol{G}_H$ are the mass, damper and spring matrix of the human limb, respectively. However, it can be shown that the damper and spring components of the human limb model are usually dominant . Accordingly, (3) can be simplified as [25]:

$$\boldsymbol{C}_H\dot{\boldsymbol{x}}+\boldsymbol{G}_H\left(\boldsymbol{x}-\boldsymbol{x}_d\right)=-\boldsymbol{f}_H. \tag{4}$$

Note that matrices $\boldsymbol{C}_H$, $\boldsymbol{G}_H$ in (4), have time-varying properties, as the human partner may modulate the damping and stiffness of his/her limb during the collaboration. Also, $\boldsymbol{x}_d$ in (4)

is the trajectory planned in the human's central nervous system which is referred to as the motion intention of the human partner, i.e. following the given desired trajectory in this paper as it is supposed that the interaction between human and robot is kinesthetic. In addition, as explained in 2.1, the objective of the paper is to design the input control $\boldsymbol{\tau}$, and the topic of the so-called human motor control is out of our scope; though interested readers can refer to [26, 27]. In particular, in this study, the human limb is treated as a system which by applying the force $\boldsymbol{f_H}$, can contribute to control of the robot states and can change its own states, accordingly.

### *2.4. Neural network approximation*

In the literature on adaptive control of robotic systems, NN are typically used for the approximation of unknown nonlinearities due to their approximation property and learning capability. It has been shown that a class of linearly parameterized NN with radial basis function (RBF) [28] can approximate an arbitrary continuous function $\boldsymbol{f}(\boldsymbol{Z}):\mathbf{R}^{q}\to\mathbf{R}$ over a compact set $\Omega_Z\subset\mathbf{R}^{q}$ to any accuracy as,

$$\boldsymbol{f}(\boldsymbol{Z})=\boldsymbol{W}^{*T}\boldsymbol{h}(\boldsymbol{Z})+\boldsymbol{\varepsilon},\ \forall\boldsymbol{Z}\in\Omega_Z, \tag{5}$$

where $\boldsymbol{Z}\in\mathbf{R}^{q}$ is the NN input vector, $\boldsymbol{W}^{*}\in\mathbf{R}^{s}$ ($\boldsymbol{s}>1$ is the NN node number) is an unknown optimal constant weight vector, and $\boldsymbol{\varepsilon}\in\mathbf{R}$ are the functional approximation errors under the ideal NN weight. The unknown error $\boldsymbol{\varepsilon}$ is bounded as $|\boldsymbol{\varepsilon}|\le\bar{\boldsymbol{\varepsilon}}<\infty$ with $\bar{\boldsymbol{\varepsilon}}$ being an unknown constant. Several applications of NN have shown that by choosing a large enough node number, $\bar{\boldsymbol{\varepsilon}}$ can be reduced to an arbitrarily small value over a compact set [29]. $\boldsymbol{h}(\boldsymbol{Z})=\left[\boldsymbol{h}_1(\boldsymbol{Z}),...,\boldsymbol{h}_s(\boldsymbol{Z})\right]^{T}\in\mathbf{R}^{s}$ are vectors of Gaussian functions and expressed as,

$$\boldsymbol{h}_i(\boldsymbol{Z})=\exp\left[\frac{-(\boldsymbol{Z}-\boldsymbol{\mu}_i)^{T}(\boldsymbol{Z}-\boldsymbol{\mu}_i)}{\boldsymbol{\rho}_i^{2}}\right], \tag{6}$$

for $\boldsymbol{i}=1,2,...,\boldsymbol{s}$, and $\boldsymbol{\mu}_i$ is the center for the $\boldsymbol{i}^{th}$ input element of the NN, and $\boldsymbol{\rho}_i$ is the variance. An approximation of $\boldsymbol{f}(\boldsymbol{Z})$ can be presented as [30],

$$\hat{\boldsymbol{f}}(\boldsymbol{Z})=\hat{\boldsymbol{W}}^{T}\boldsymbol{h}(\boldsymbol{Z}), \tag{7}$$

where $\hat{\boldsymbol{W}}\in\mathbf{R}^{s}$ is the vector of estimation of the corresponding optimal weights $\boldsymbol{W}^{*}$ defined as,

$$\boldsymbol{W}^{*}:=\arg\min_{\boldsymbol{W}\in\mathbf{R}^{s}}\left\{\sup_{\boldsymbol{Z}\subset\Omega_Z}\left|\boldsymbol{f}(\boldsymbol{Z})-\boldsymbol{W}^{T}\boldsymbol{h}(\boldsymbol{Z})\right|\right\}. \tag{8}$$

### *2.5. Definitions*

**Definition 1** (Barrier Lyapunov Function) [31]. A barrier Lyapunov function (BLF) is a positive definite continuous scalar function $\boldsymbol{V}(\boldsymbol{x})$ which is defined with respect to the system $\dot{\boldsymbol{x}}=\boldsymbol{f}(\boldsymbol{x})$ on an open region $\Upsilon$ containing the origin, such that it has continuous first order partial derivatives within all $\Upsilon$, and $\boldsymbol{V}(\boldsymbol{x})\to\infty$, as $\boldsymbol{x}$ approaches the boundary of the region

$\Upsilon$, and satisfies $V(x(t)) \le \varpi, \forall t \ge 0$ along the solution of $\dot{x} = f(x)$ for $x(0) \in \Upsilon$, and some positive constant $\varpi$.

**Definition 2 (**Semiglobally Uniformly Ultimately Bounded) [32]. The solution of a system $z(t)$ is Semiglobally Uniformly Ultimately Bounded (SGUUB) if, there exists a number $T(\mathrm{K}, z(t_0))$, and a $\mathrm{K} > 0$ such that for any compact set $\Omega_s$ and all $z(t_0) \in \Omega_s$, $\|z(t)\| \le \mathrm{K}$ for all $t \ge t_0 + T$.

### *2.6. Lemmas*

**Lemma 1** [33]. The following inequality holds for all $|\chi| < 1$:

$$\ln \frac{1}{1-\chi^2} < \frac{\chi^2}{1-\chi^2}.$$

**Lemma 2** [30]. Consider a positive function given by,

$$V(t) = \frac{1}{2}\zeta^T(t)\Xi(t)\zeta(t) + \frac{1}{2}\tilde{\omega}^T(t)\Pi^{-1}(t)\tilde{\omega}(t), \tag{9}$$

where $\zeta(t) = \chi(t) - \chi_d(t)$, and $\tilde{\omega}(t) = \omega^* - \hat{\omega}(t)$ with constants $\omega^* \in \mathbf{R}^m$, and $\hat{\omega}(t) \in \mathbf{R}^m$, $\chi(t) \in \mathbf{R}^n$, $\chi_d(t) \in \Omega_d \subset \mathbf{R}^n$; $\Xi(t) = \Xi^T(t) > 0$ and $\Pi(t) = \Pi^T(t) > 0$ are dimensionally compatible matrices. If the following inequality holds:

$$\dot{V}(t) \le -\alpha_1 V(t) + \alpha_2, \tag{10}$$

where $\alpha_1$, and $\alpha_2$ are positive constants, then, given any initial compact set defined by,

$$\Omega_0 := \left\{ \chi(0), \chi_d(0), \hat{\omega}(0) \middle| \chi(0), \hat{\omega}(0) \text{ finite}, \chi_d(0) \in \Omega_d \right\}, \tag{11}$$

the states and weights in the closed-loop system will remain in the compact set defined by,

$$\Omega := \left\{ \begin{array}{l} \chi(t), \hat{\omega}(t) \middle| \|\chi(t)\| \le \mu_{\zeta_m} + \max\limits_{\tau \in [0,t]} \left\{ \|\chi_d(\tau)\| \right\}, \\ \chi_d(t) \in \Omega_d, \|\hat{\omega}\| \le \mu_{\tilde{\omega}_m} + \|\omega^*\| \end{array} \right\}, \tag{12}$$

and will eventually converge to the compact sets defined by,

$$\Omega_s := \left\{ \chi(t), \hat{\omega}(t) \middle| \lim_{x \to \infty} \|\zeta(t)\| = \mu_\zeta, \lim_{x \to \infty} \|\tilde{\omega}\| = \mu_{\tilde{\omega}} \right\}, \tag{13}$$

where constants $\mu_{\zeta_m} = \sqrt{\left(2V(0) + 2\alpha_2/\alpha_1\right)/\lambda_{\Xi_{\min}}}$, $\mu_{\tilde{\omega}_m} = \sqrt{\left(2V(0) + 2\alpha_2/\alpha_1\right)/\lambda_{\Pi^{-1}{}_{\min}}}$, $\mu_\zeta = \sqrt{2\alpha_2/\alpha_1\lambda_{\Xi_{\min}}}$, and $\mu_{\tilde{\omega}} = \sqrt{2\alpha_2/\alpha_1\lambda_{\Pi^{-1}{}_{\min}}}$.

## 3. HRI control structure

### *3.1. Assistive HRI and overall structure of the proposed method*

A preview of the overall structure of the proposed assistive HRI system is presented in this section. The developed control architecture includes two control loops, namely an inner-loop, and an outer-loop. First, the neural adaptive impedance controller is designed in the inner loop to make the unknown nonlinear robot follow the reference trajectory in the task space, while the stability of the closed-loop system is guaranteed. Then, the neural outer-loop controller is designed, which by minimizing the overall human–robot interaction performance, updates parameters of the impedance model. Accordingly, with the inner-loop control, the problem of unknown dynamics of the robot can be handled while the model tracking error is going to be close to zero. In contrast, in the outer-loop control, impedance parameters are assigned to make an unknown reference trajectory track the desired trajectory, while minimizing the interaction force.

The overall schematic of the proposed two-loop control structure is shown in Fig. 1.

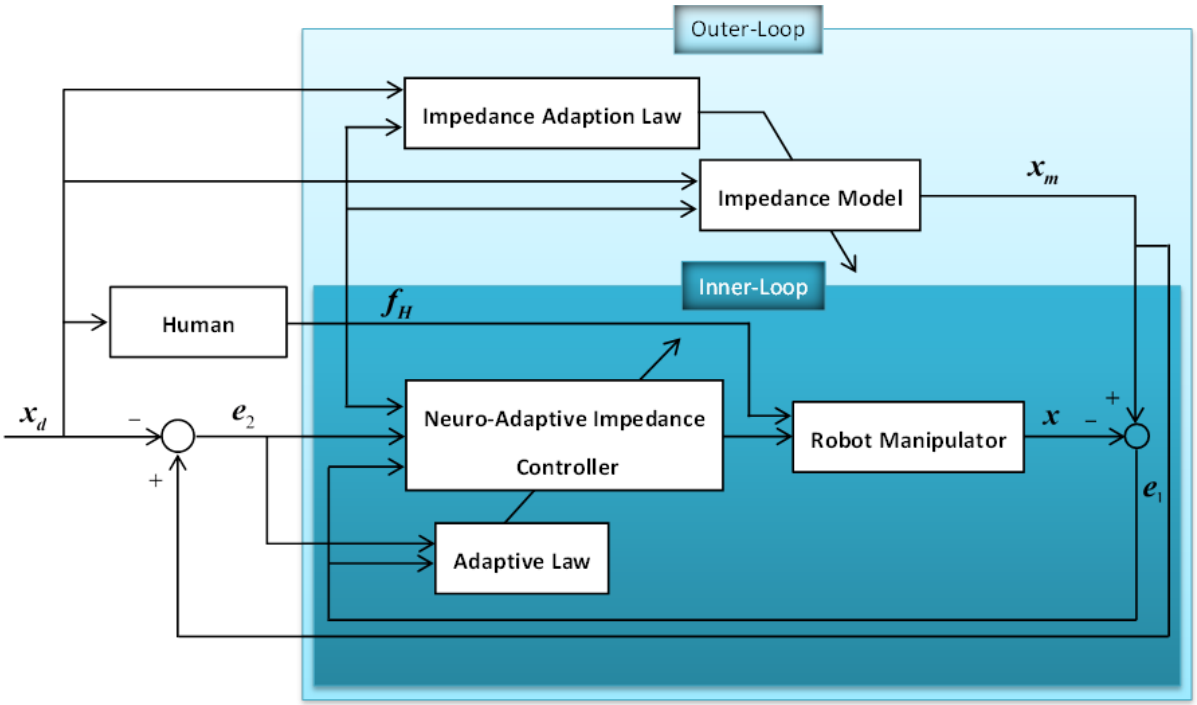


Figure 1. Overall control design for assistive HRI system.

### *3.2. Neural adaptive impedance inner-loop control design*

**Design objective.** For the given robot dynamics (1), the target impedance model (2), and the human limb dynamics (4), find, if possible, the input control $\boldsymbol{\tau}$ such that unknown robot dynamics behave like a prescribed robot impedance model, as close as possible. Accordingly, neuro-adaptive impedance control can be achieved by properly designing the inner-loop control.

#### *3.2.1. Controller design and stability analysis*

To satisfy the objective design of this section, we aimed to handle the tracking control task by properly bounding the model-following error variable $\boldsymbol{e}_1 = \boldsymbol{x}_m - \boldsymbol{x}$. Also, to cope with the uncertain robot dynamics problem, the RBF NN are used to approximate the unknown parameters. Consider the neural impedance adaptive control law as,

$$\boldsymbol{\tau} = -\boldsymbol{f}_H + \hat{\boldsymbol{W}}_1^T \boldsymbol{h}_1 + \boldsymbol{K}_s \boldsymbol{e}_s + \boldsymbol{e}_1, \tag{14}$$

where $\boldsymbol{e}_s = \dot{\boldsymbol{e}}_1 + \boldsymbol{K}_1 \boldsymbol{e}_1$, and $\boldsymbol{K}_1$, and $\boldsymbol{K}_s$ are positive control gains, and $\hat{\boldsymbol{W}}_1$ is an estimation of ideal weights $\boldsymbol{W}_1^*$ of the NN. Using the NN explained in subsection 2.4, $\hat{\boldsymbol{W}}_1^T \boldsymbol{h}_1$ is used to approximate,

$$\boldsymbol{M}\ddot{\boldsymbol{x}}_r + \boldsymbol{C}\dot{\boldsymbol{x}}_r + \boldsymbol{G} = \boldsymbol{W}_1^{*T} \boldsymbol{h}_1 + \boldsymbol{\varepsilon}_1, \tag{15}$$

where $\dot{\boldsymbol{x}}_r = \dot{\boldsymbol{x}}_m + \boldsymbol{K}_1 \boldsymbol{e}_1$, and $\boldsymbol{\varepsilon}_1$ is the estimation error and bounded with unknown positive constant $\bar{\boldsymbol{\varepsilon}}_1$. The update rule for the NN weights is given by,

$$\dot{\hat{\boldsymbol{W}}}_1 = \Gamma\left(\boldsymbol{h}_1 \boldsymbol{e}_s - \sigma \hat{\boldsymbol{W}}_1\right), \tag{16}$$

where $\Gamma = \Gamma^T > 0$, and $\sigma > 0$.

**Theorem 1.** Consider the robotic manipulator dynamics (1) satisfying Property 1, and the prescribed robot impedance model (2). Let the actual control input be given by (14). Let the NN weight updating rule be chosen as (16). Then, for any initial compact set, the error signals $\boldsymbol{e}_1$ and $\boldsymbol{e}_s$, and the NN estimated weights $\tilde{\boldsymbol{W}}_1$ are SGUUB.

**Proof.** Consider the Lyapunov candidate function as,

$$\boldsymbol{V} = \frac{1}{2}\boldsymbol{e}_1^T \boldsymbol{e}_1 + \frac{1}{2}\boldsymbol{e}_s^T \boldsymbol{M} \boldsymbol{e}_s + \frac{1}{2}\Gamma^{-1} \tilde{\boldsymbol{W}}_1^T \tilde{\boldsymbol{W}}_1. \tag{17}$$

Differentiating Lyapunov function $\boldsymbol{V}$ with respect to time, gives,

$$\begin{aligned} \dot{\boldsymbol{V}} &= \boldsymbol{e}_1^T \dot{\boldsymbol{e}}_1 + \boldsymbol{e}_s^T \boldsymbol{M} \dot{\boldsymbol{e}}_s + \frac{1}{2}\boldsymbol{e}_s^T \dot{\boldsymbol{M}} \boldsymbol{e}_s + \Gamma^{-1} \tilde{\boldsymbol{W}}_1^T \dot{\tilde{\boldsymbol{W}}}_1 \\ &= \boldsymbol{e}_1^T \left(\dot{\boldsymbol{e}}_1 - \boldsymbol{K}_1 \boldsymbol{e}_1 + \boldsymbol{K}_1 \boldsymbol{e}_1\right) + \boldsymbol{e}_s^T \left(-\boldsymbol{\tau} - \boldsymbol{f}_H + \boldsymbol{C}\dot{\boldsymbol{x}} + \boldsymbol{G} + \boldsymbol{M}\ddot{\boldsymbol{x}}_r + \frac{1}{2}\dot{\boldsymbol{M}}\boldsymbol{e}_s\right) + \Gamma^{-1} \tilde{\boldsymbol{W}}_1^T \dot{\tilde{\boldsymbol{W}}}_1. \end{aligned} \tag{18}$$

Noting $\dot{\tilde{\boldsymbol{W}}}_1 = -\dot{\hat{\boldsymbol{W}}}_1$, then using Property 1, (18) can be written as,

$$\dot{\boldsymbol{V}} = -\boldsymbol{e}_1^T \boldsymbol{K}_1 \boldsymbol{e}_1 + \boldsymbol{e}_1^T \boldsymbol{e}_s + \boldsymbol{e}_s^T \left(-\boldsymbol{\tau} - \boldsymbol{f}_H + \boldsymbol{C}\dot{\boldsymbol{x}}_r + \boldsymbol{G} + \boldsymbol{M}\ddot{\boldsymbol{x}}_r\right) - \Gamma^{-1} \tilde{\boldsymbol{W}}_1^T \dot{\hat{\boldsymbol{W}}}_1. \tag{19}$$

Substituting (14), (15), and (16), into (19) one can obtain,

$$\dot{\boldsymbol{V}} = -\boldsymbol{e}_1^T \boldsymbol{K}_1 \boldsymbol{e}_1 - \boldsymbol{e}_s^T \boldsymbol{K}_s \boldsymbol{e}_s + \boldsymbol{e}_s^T \tilde{\boldsymbol{W}}_1^T \boldsymbol{h}_1 + \boldsymbol{e}_s^T \boldsymbol{\varepsilon}_1 - \tilde{\boldsymbol{W}}_1^T \left(\boldsymbol{h}_1 \boldsymbol{e}_s - \sigma \hat{\boldsymbol{W}}_1\right). \tag{20}$$

Noting $\boldsymbol{e}_s^T \tilde{\boldsymbol{W}}_1^T \boldsymbol{h}_1 = \boldsymbol{h}_1^T \tilde{\boldsymbol{W}}_1 \boldsymbol{e}_s = \tilde{\boldsymbol{W}}_1^T \boldsymbol{h}_1 \boldsymbol{e}_s$, and $\tilde{\boldsymbol{W}}_1^T \hat{\boldsymbol{W}}_1 = \tilde{\boldsymbol{W}}_1^T \boldsymbol{W}_1^* - \tilde{\boldsymbol{W}}_1^T \tilde{\boldsymbol{W}}_1$, we have,

$$\dot{\boldsymbol{V}} = -\boldsymbol{e}_1^T \boldsymbol{K}_1 \boldsymbol{e}_1 - \boldsymbol{e}_s^T \boldsymbol{K}_s \boldsymbol{e}_s + \boldsymbol{e}_s^T \boldsymbol{\varepsilon}_1 + \sigma \tilde{\boldsymbol{W}}_1^T \boldsymbol{W}_1^* - \sigma \tilde{\boldsymbol{W}}_1^T \tilde{\boldsymbol{W}}_1. \tag{21}$$

Applying Young's inequality , we have $\boldsymbol{e}_s^T \boldsymbol{\varepsilon}_1 \le 1/2\, \boldsymbol{e}_s^T \boldsymbol{e}_s + 1/2\, \boldsymbol{\varepsilon}_1^T \boldsymbol{\varepsilon}_1$, and further $\sigma \tilde{\boldsymbol{W}}_1^T \boldsymbol{W}_1^* \le \sigma/2\, \tilde{\boldsymbol{W}}_1^T \tilde{\boldsymbol{W}}_1 + \sigma/2\, \boldsymbol{W}_1^{*T} \boldsymbol{W}_1^*$ , then (21) can be formed as,

$$\dot{\boldsymbol{V}} \le -\boldsymbol{e}_1^{\,T}\boldsymbol{K}_1\boldsymbol{e}_1 - \boldsymbol{e}_s^{\,T}\left(\boldsymbol{K}_s - \boldsymbol{I}/2\right)\boldsymbol{e}_s - 1/2\,\sigma\tilde{\boldsymbol{W}}_1^{\,T}\tilde{\boldsymbol{W}}_1 + 1/2\,\sigma\left\|\boldsymbol{W}_1^{*}\right\|^2 + 1/2\left\|\bar{\boldsymbol{\varepsilon}}_1\right\|^2 \le -\alpha_1\boldsymbol{V} + \alpha_2, \quad (22)$$

where, $\alpha_1 = \min\left(2\boldsymbol{K}_1, \lambda_{\min}\left(2\boldsymbol{K}_s - \boldsymbol{I}\right)/\lambda_{\max}\left(\boldsymbol{M}\right), \sigma/\lambda_{\max}\left(\Gamma^{-1}\right)\right)$ and $\alpha_2 = 1/2\left(\sigma\left\|\boldsymbol{W}_1^{*}\right\|^2 + \left\|\bar{\boldsymbol{\varepsilon}}_1\right\|^2\right)$. According to Lemma 2, if $2\boldsymbol{K}_s - \boldsymbol{I}_{n\times n} > 0$, where $\boldsymbol{I}_{n\times n}$ is an $n\times n$ identity matrix then, signals $\boldsymbol{e}_1$, $\boldsymbol{e}_s$ ,and the NN weights in the closed-loop signals will remain SGUUB. For completeness, multiplying inequality (10) by $\exp\left(\alpha_1 t\right)$ and then, integrating it, one can obtain,

$$\begin{aligned} \boldsymbol{V}(t) &\le \left(\boldsymbol{V}(0) - \frac{\alpha_2}{\alpha_1}\right)\exp\left(-\alpha_1 t\right) + \frac{\alpha_2}{\alpha_1} \\ &\le \boldsymbol{V}(0) + \frac{\alpha_2}{\alpha_1}, \qquad \forall t > 0. \end{aligned} \quad (23)$$

Therefore, signals $\boldsymbol{e}_1$, $\boldsymbol{e}_s$, and $\tilde{\boldsymbol{W}}_1$ remain in the compact set defined by $\Omega_e := \left\{\Theta \middle\| \|\Theta\| \le \mu_e\right\}$, and will eventually and exponentially converge to the compact set defined by $\Omega_{eU} := \left\{\Theta \middle\| \|\Theta\| \le \mu_{eU}\right\}$, where $\mu_e = \sqrt{2\left(\boldsymbol{V}(0) + \alpha_1/\alpha_2\right)}$, and $\mu_{eU} = \sqrt{2\alpha_1/\alpha_2}$. Accordingly, we can understand that choosing different initial conditions can affect the bounding compact sets, but not the steady state compact set. Also, it is clear that by reducing $\alpha_1$, or increasing $\alpha_2$ one can make the size of $\mu_e$, or $\mu_{eU}$ very small. However, choosing the control parameters should be done carefully as taking a large $\boldsymbol{K}_1$ may lead to increase of motor input voltage $\tau$, or choosing small $\sigma$ can result in producing large NN weights. ■

**Remark 3.** Compared to controllers that developed adaptive impedance control proposed in [34, 35], in the present controller, the linearly-in-parameter assumption on robot dynamics are removed. Also, unknown terms in (15), do not contain the robot impedance parameters $\boldsymbol{M}_r$, $\boldsymbol{B}_r$, and $\boldsymbol{K}_r$. Thus, NN will only estimate robot dynamics $\boldsymbol{M}$ ,$\boldsymbol{C}$, and $\boldsymbol{G}$, but not the impedance model. By that means, impedance updating can be executed in the outer-loop controller independent from robot dynamics. In addition, with respect to the previous works in [17, 18] which only considered a model-following error in the inner-loop controller, in the presented inner-loop control design, both trajectory-following error and model-following error are handled. By that means, the outer-loop controller assistive scenario can be performed by only considering the human-robot interaction force as the cost function to be minimized.

### *3.2.2. Controller modification based on barrier Lyapunov function*

Motivated by increasing the safety in human-robot interaction, we present constrained control by modifying the presented controller in the previous section. By that means, hard constraints are imposed on the movements to minimize the risk of human partner injuries. To this end, we utilized the barrier Lyapunov function to prevent constraint violations. Note that using the BLF during the system control design, by ensuring that the errors remain bounded in the certain set, can improve the functionality of the NN-associated unit [36]. The logarithm-type BLF candidate is chosen as $\boldsymbol{V}_c = 0.5\log\left(\kappa^2/\kappa^2 - \aleph^2\right)$ [31] where $\kappa$ is

the constraint, and $\aleph$ is the variable to be constrained.

The structure of the presented inner-loop control design is shown in Fig. 2.

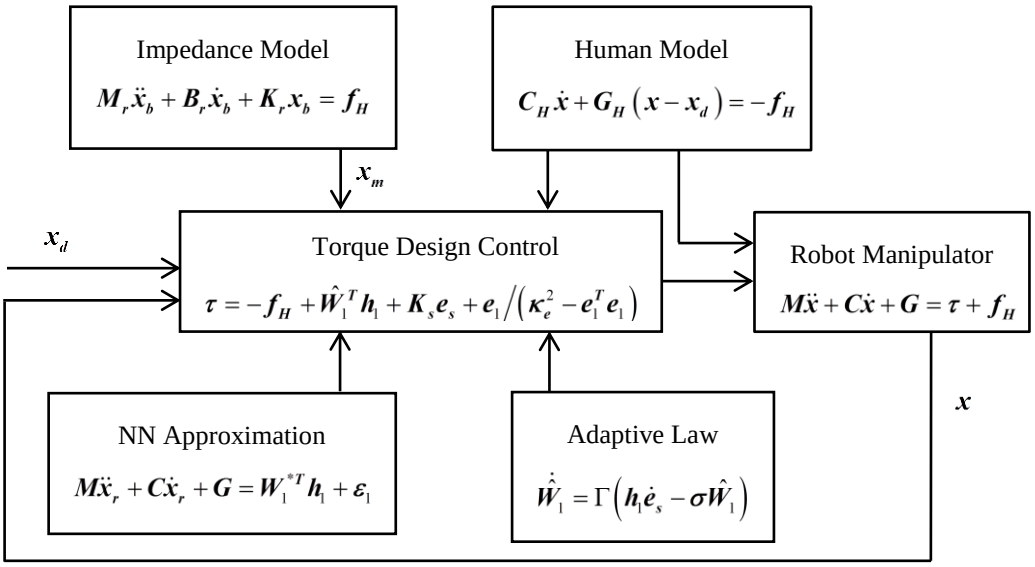


Figure 2. The structure of the inner-loop control design.

**Theorem 2.** For the robot system defined by (1), under the hypotheses of Theorem 1, let the NN weight tuning be given by (16), with the initial conditions, then provided that $\|e_1(0)\| < \kappa_e$ with $\kappa_e$ being constant, then the SGUUB tracking is achieved while tracking error $e_1(t)$ remains constrained, for all $t > 0$, as $|e_1(t)| < \kappa_e$ if the control input is given by,

$$\tau = -f_H + \hat{W}_1^T h_1 + K_s e_s + \frac{e_1}{\kappa_e^2 - e_1^T e_1}. \tag{24}$$

**Proof.** Choose the Lyapunov candidate function including the barrier term as,

$$V = \frac{1}{2}\log\left(\frac{\kappa_e^2}{\kappa_e^2 - e_1^T e_1}\right) + \frac{1}{2} e_s^T M e_s + \frac{1}{2}\Gamma^{-1}\tilde{W}_1^T\tilde{W}_1. \tag{25}$$

Time differentiation of (25), with consideration of Property 1 and $\dot{\tilde{W}}_1 = -\dot{\hat{W}}_1$, can give,

$$\begin{aligned}\dot{V} &= \frac{e_1^T}{\kappa_e^2 - e_1^T e_1}(\dot{e}_1 - K_1 e_1 + K_1 e_1) + e_s^T\left(-\tau - f_H + C\dot{x} + G + M\ddot{x}_r + \frac{1}{2}\dot{M}e_s\right) + \Gamma^{-1}\tilde{W}_1^T\dot{\tilde{W}}_1 \\ &= -K_1\frac{e_1^T e_1}{\kappa_e^2 - e_1^T e_1} + \frac{e_1^T}{\kappa_e^2 - e_1^T e_1} e_s + e_s^T(-\tau - f_H + C\dot{x}_r + G + M\ddot{x}_r) - \Gamma^{-1}\tilde{W}_1^T\dot{\hat{W}}_1.\end{aligned} \tag{26}$$

Substituting approximation (15), updating rule (16), control (24) into (26) one can obtain,

$$\dot{V} = -K_1\frac{e_1^T e_1}{\kappa_e^2 - e_1^T e_1} - e_s^T K_s e_s + e_s^T\tilde{W}_1^T h_1 + e_s^T\varepsilon_1 - \tilde{W}_1^T(h_1 e_s - \sigma\hat{W}_1). \tag{27}$$

Now considering Lemma 1, and following a similar analysis procedure as in the proof of Theorem 1, one can finally establish that $\dot{V} \le -\alpha_1 V + \alpha_2$ with the same $\alpha_1$ and $\alpha_2$ as those obtained in the proof of Theorem 1. Then, using the Lemma 2, SGUUB of the closed-loop system can be obtained.

The proof of $|e_1(t)| < \kappa_e, \forall t \ge 0$ is presented by contradiction. Assume that there exists some $t = \tau$ such that the tracking error $|e_1(\tau)|$ grows to the bound $\kappa_e$ for the first time. Substitute $|e_1(\tau)| = \kappa_e$ into the BLF (25), then $V$ becomes unbounded which contradicts the boundness of the Lyapunov function as in (23). It is consequently proved that error $|e_1(\tau)|$ cannot grow to its bound $\kappa_e$ i.e. $|e_1(t)| < \kappa_e, \forall t \ge 0$. ■

### *3.3. Outer-loop neural network based impedance adaption*

**Design objective.** For the given inner-loop design in the Section 3.2.2., find the critical robot impedance parameters $M_r$, $B_r$, and $K_r$ to assist the human partner to perform a task with minimum control effort $f_H$, meanwhile the reference model tracks a given desired trajectory, in the task space, as closely as possible.

To achieve the control objective, first stability guarantee of the reference model is considered, then the adaptive NN-based on-line estimation method using the backpropagation algorithm is proposed. The result is to make the trajectory-following error, $e_2$, and interaction force, $f_H$, as small as possible by updating the critical impedance parameters.

#### *3.3.1. Stability of the robot reference model*

The adaptive controller presented in the previous section is tracking the reference model (2), and thus makes the closed-loop dynamics of the robot system (1) similar to the reference model. To guarantee the system stability, all poles of the reference model must have negative real parts. Accordingly, as the robot dynamics can be expressed by a second-order differential equation, the model should have two poles on the left half of the complex plane . To make sure that the reference model (2) is stable, the impedance parameter should be selected, such that the polynomial,

$$P(S) = M_r S^2 + B_r S + K_r, \tag{28}$$

is a Hurwitz polynomial, where $S$ is the Laplace operator. To satisfy the condition that the polynomial (28) is Hurwitz, we select $M_r = \mathrm{diag}[M_{r,j}]$, $B_r = \mathrm{diag}[B_{r,j}]$, and $K_r = \mathrm{diag}[K_{r,j}]$ for $j = 1, 2$ so that all eigenvalues of (28) have negative real parts. For positive $\lambda_{1,j}$, and $\lambda_{2,j}$ in,

$$(\lambda_{1,j} S + \lambda_{2,j})^2 = 0, \tag{29}$$

we have a double root at $-\lambda_{2,j}/\lambda_{1,j}$. Without loss of generality, in (29) let $\lambda_{1,j} = 1$, then we have $S^2 + 2\lambda_{2,j} S + {\lambda_{2,j}}^2 = 0$, and it has a double root at $-\lambda_{2,j}$ for all $\lambda_{2,j} \in \mathbf{R}^+$. Accordingly,

comparing (28), and (29), and using the above simplification, to make (28) be the Hurwitz polynomial, we can choose $\boldsymbol{B}_{r,j}=2\lambda_{2,j}$, $\boldsymbol{K}_{r,j}=\lambda_{2,j}{}^{2}$ with $\boldsymbol{M}_{r,j}=1$.

### *3.3.2. Assistive impedance adaption*

The aim of this section is to find impedance parameters $\boldsymbol{B}_r$, and $\boldsymbol{K}_r$ so that the HRI performance is optimized. Using the RBF-NN damping matrix $\boldsymbol{B}_r$, its estimation can be represented as,

$$\begin{aligned}\boldsymbol{B}_{r,i}&=\boldsymbol{W}_{2i}^{*T}\boldsymbol{h}_{2,i}+\boldsymbol{\varepsilon}_{2i},\\ \hat{\boldsymbol{B}}_{r,i}&=\hat{\boldsymbol{W}}_{2i}{}^{T}\boldsymbol{h}_{2,i},\end{aligned}\tag{30}$$

where $(\cdot)_i$ is the $i^{\text{th}}$ component of $(\cdot)$, $\hat{\boldsymbol{W}}_{2i}$ is the estimation of the ideal weight $\boldsymbol{W}_{2i}^{*}$, $\boldsymbol{h}_{2,i}$ is the basis function vector, and $\boldsymbol{\varepsilon}_2$ is the estimation error. Note that it is known that $\boldsymbol{\varepsilon}_{2i}$ can be made arbitrarily small if the number of basis functions is sufficiently large [37]. In this study, $\hat{\boldsymbol{W}}_{2i}$ is obtained by the backpropagation algorithm [38]. In order to achieve assistive human-robot interaction, we choose the weight updating law to minimize the objective function $\Xi_i$, which is defined as,

$$\Xi_i=\frac{1}{2}\boldsymbol{r}_1\boldsymbol{f}_{H,i}{}^{2}+\frac{1}{2}\boldsymbol{r}_2\boldsymbol{e}_{2,i}{}^{2},\tag{31}$$

where $\boldsymbol{r}_1$ and $\boldsymbol{r}_2$ are waiting coefficients. Damping matrix $\boldsymbol{B}_{r,i}$ can be obtained by updating weights $\hat{\boldsymbol{W}}_{2i}$ according to the steepest descent method as,

$$\dot{\hat{\boldsymbol{W}}}_{2i}(\boldsymbol{t})=-\eta_i\frac{\partial\Xi_i}{\partial\hat{\boldsymbol{W}}_{2i}},\tag{32}$$

where $\eta\in(0,1)$ is the learning rate. According to (30), (31) and (2), we have,

$$\begin{aligned}\dot{\hat{\boldsymbol{W}}}_{2i}&=-\frac{1}{2}\eta_i\left(\boldsymbol{r}_1\frac{\partial\boldsymbol{f}_{H,i}{}^{2}}{\partial\hat{\boldsymbol{W}}_{2i}}+\boldsymbol{r}_2\frac{\partial\boldsymbol{e}_{2,i}{}^{2}}{\partial\hat{\boldsymbol{W}}_{2i}}\right)\\ \dot{\hat{\boldsymbol{W}}}_{2i}&=-\frac{1}{2}\eta_i\boldsymbol{r}_1\left(\frac{\partial\boldsymbol{f}_{H,i}{}^{2}}{\partial\boldsymbol{f}_{H,i}}\right)\left(\frac{\partial\boldsymbol{f}_{H,i}}{\partial\boldsymbol{B}_{r,i}}\right)\left(\frac{\partial\boldsymbol{B}_{r,i}}{\partial\hat{\boldsymbol{W}}_{2i}}\right)-\frac{1}{2}\eta_i\boldsymbol{r}_2\left(\frac{\partial\boldsymbol{e}_{2,i}{}^{2}}{\partial\boldsymbol{e}_{2,i}}\right)\left(\frac{\partial\boldsymbol{e}_{2,i}}{\partial\boldsymbol{B}_{r,i}}\right)\left(\frac{\partial\boldsymbol{B}_{r,i}}{\partial\hat{\boldsymbol{W}}_{2i}}\right)\\ &=-\eta_i\boldsymbol{r}_1\boldsymbol{f}_{H,i}\dot{\boldsymbol{x}}_{b,i}\boldsymbol{h}_{2,i}+\eta_i\boldsymbol{r}_2\boldsymbol{e}_{2,i}\left(\dot{\boldsymbol{x}}_{b,i}/\boldsymbol{K}_{r,i}\right)\boldsymbol{h}_{2,i},\end{aligned}\tag{33}$$

then, the updating law of $\hat{\boldsymbol{W}}_{2i}$ can be obtained as,

$$\hat{\boldsymbol{W}}_{2i}(\boldsymbol{t})=\hat{\boldsymbol{W}}_{2i}(0)-\eta_i\int_0^t\left[\boldsymbol{r}_1\boldsymbol{f}_{H,i}\dot{\boldsymbol{x}}_{b,i}\boldsymbol{h}_{2,i}-\boldsymbol{r}_2\boldsymbol{e}_{2,i}\left(\dot{\boldsymbol{x}}_{b,i}/\boldsymbol{K}_{r,i}\right)\boldsymbol{h}_{2,i}\right]\boldsymbol{dw}.\tag{34}$$

Accordingly, using (30), and (34) we can obtain the estimated damping matrix $\hat{\boldsymbol{B}}_{r,i}$. Then considering $\hat{\boldsymbol{B}}_{r,i}=2\lambda_{2,i}$, we can obtain the amount of constant $\lambda_{2,i}$, and consequently estimate

$\boldsymbol{K}_{r,i}$ as $\hat{\boldsymbol{K}}_{r,i} = \boldsymbol{\lambda}_{2,i}{}^2$. By that means, the impedance parameters $\boldsymbol{B}_r$ and $\boldsymbol{K}_r$ can be updated in order to obtain assistive human-robot interaction.

The overall algorithm for updating the impedance parameters are summarized in Algorithm 1.

Algorithm 1: Updating of Impedance Parameters

**Input**: The error variable $\dot{x}_b$, the interaction force $f_H$, and NN input vector $Z_2$.

**Output:** Estimated impedance parameters $\hat{B}_r$, and $\hat{K}_r$.

**begin**

Set the cost function (31) to find the optimal values of the impedance parameters. Set the proper Gaussian function $h_2$. Initialize the estimated NN weights $\hat{W}_2$. Set the learning rate $\eta$.

**while** $t < t_f$, where $t_f$ is the termination time, **do**

Collect the error variable $\dot{x}_b$, and the interaction force $f_H$.

Calculate $\hat{W}_2$ by solving (34).

Obtain the damping matrix $\hat{B}_r$ as in (30).

Obtain the value of $\lambda_2$ as $\lambda_2 = \hat{B}_r/2$.

Obtain the stiffness matrix $\hat{K}_r = \lambda_2{}^2$.

Form the robot impedance at (2).

## 4. Simulation study

In this section, the effectiveness of the proposed control scheme is validated by numerical simulations. The particular objective is to verify if employing the designed assistive neural adaptive impedance controller can result in stable tracking while updating impedance parameters. A two-link robot manipulator in the vertical plane is used for the simulation. Two cases are considered to evaluate the performance of the proposed method. In the first case, the proposed assistive HRI control is verified via numerical simulation. In the second simulation, the comparison is performed between the presented control and the impedance control with the fixed impedance model parameters. Then, using appropriate criteria the performance of the controllers is compared in a quantified manner.

Physical robot parameters are chosen as the length of links $\boldsymbol{L}_1 = \boldsymbol{L}_2 = 1\text{m}$, and masses of links $\boldsymbol{m}_1 = \boldsymbol{m}_2 = 3$ kg. The gravitational acceleration is $\boldsymbol{g} = 9.81\boldsymbol{m}/\boldsymbol{s}^2$. The desired trajectory in the Cartesian space is chosen such that the robot follows a circle centred at $\boldsymbol{x}_c = [1,1]^T \boldsymbol{m}$ with a radius of $\boldsymbol{r} = 0.5\boldsymbol{m}$, namely we choose $\boldsymbol{x}_d = \left[1+\frac{1}{2}\cos(\boldsymbol{t}), 1+\frac{1}{2}\sin(\boldsymbol{t})\right]^T \boldsymbol{m}$. The initial condition of the system in the task space is considered as $\boldsymbol{x}(0) = [1.1, 0.6]^T \boldsymbol{m}$, and $\dot{\boldsymbol{x}}(0) = [0,0]^T \boldsymbol{m}/\boldsymbol{s}$. The control algorithm as presented in Theorem 2 is utilized where the control parameters are selected as $\boldsymbol{K}_1 = \text{diag}\{[10,10]\}$, $\boldsymbol{K}_s = \text{diag}\{[200,200]\}$, $\Gamma = [1;1]$,

$\sigma = [0.02; 0.02]$, $r_1 = 1$, $r_2 = 5$ and $\eta_i = 0.45$ for $i = 1, 2$. We also use RBF NN with $s = 20$ nodes on each hidden layer. Also, to obtain $h_1 = h_1(Z_1)$ the input vector $Z_1 \in \mathbf{R}^{n\times 6}$ is chosen as $Z_1 = \left[e_1^T, e_2^T, \dot{e}_1^T, \dot{x}_r^T, \ddot{x}_r^T, e_s^T\right]$, and to obtain $h_2 = h_2(Z_2)$, we choose input vector $Z_2 \in \mathbf{R}^{n\times 5}$ as $Z_2 = \left[e_1^T, e_2^T, \dot{x}_b^T, \dot{e}_1^T, f_H^T\right]$. Other parameters used in NN approximation are $\rho_{1i} = 1$, $\rho_{2i} = 10$, $\hat{W}_{1i}(0) = 0$, $\hat{W}_{2i}(0) = 2$, and centers $\mu_i$ evenly distributed in the span of input space $[-1.5, 1.5]$ for $i = 1, 2, ..., s$. We assumed that the impedance parameters of the human arm are diagonal [19], and set as a function of $\dot{x}$ as $C_H = K_{in}C_h$, and $G_H = K_{in}G_h$ with $K_{in} = \left(\exp\left(m^2t^2\right) - 1\right) / \exp\left(m^2t^2\right)$, $C_h = \text{diag}\left\{\left[21 - 20\sin\left(\dot{x}_1\right), 21 - 20\sin\left(\dot{x}_2\right)\right]\right\}$, and $G_h = \text{diag}\left\{\left[201 - 200\sin\left(\dot{x}_1\right), 201 - 200\sin\left(\dot{x}_2\right)\right]\right\}$. Noting that the integrative function $K_{in}$ is introduced in this paper to prevent sudden jumping of the interaction force $f_H$. By that means $f_H$ can be gradually increased at the beginning of the interactive HRI. In this simulation, the incremental rate $m$ is chosen as $m = 0.3$. Simulation results are shown in Figures 3 and 4.

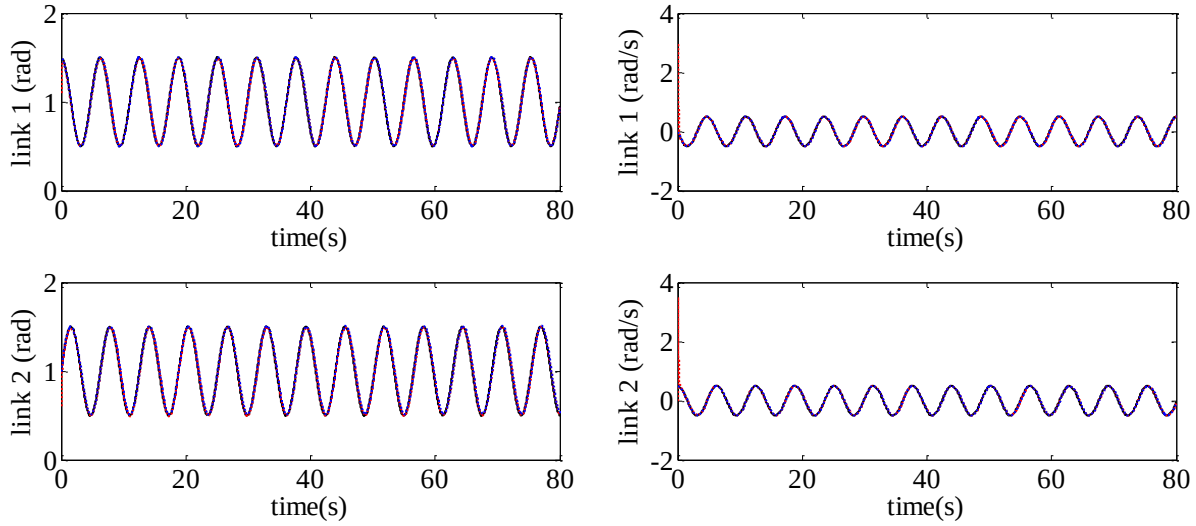


a) The trajectory of positions: the desired signal (black) versus the actual signal (red), and the reference signal (blue).

b) The trajectory of velocities: the desired signal (black) versus the actual signal (red), and the reference signal (blue).

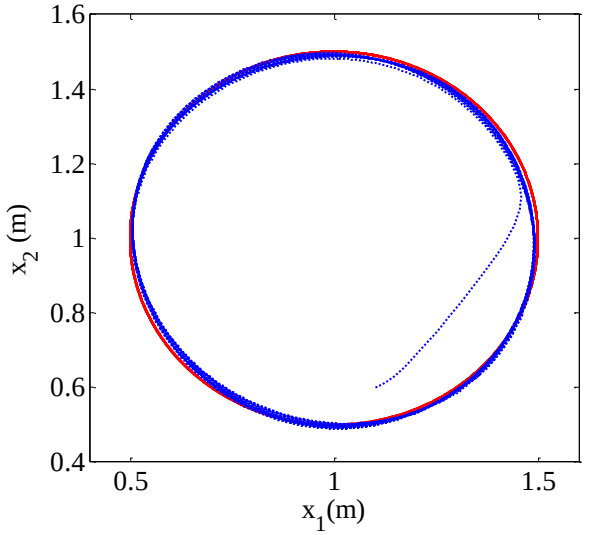


c) The trajectory of the end-effector in the Cartesian space: the desired signal (red) versus the actual signal (blue).

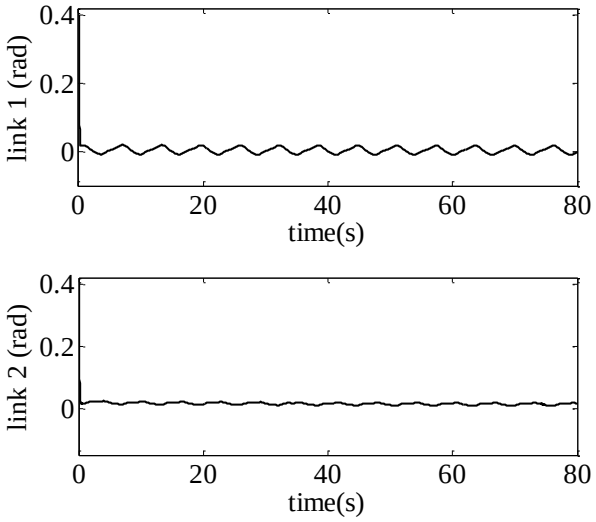


d) The trajectory of the model-following error.

Figure 3. Tracking performance of the system using the proposed control.

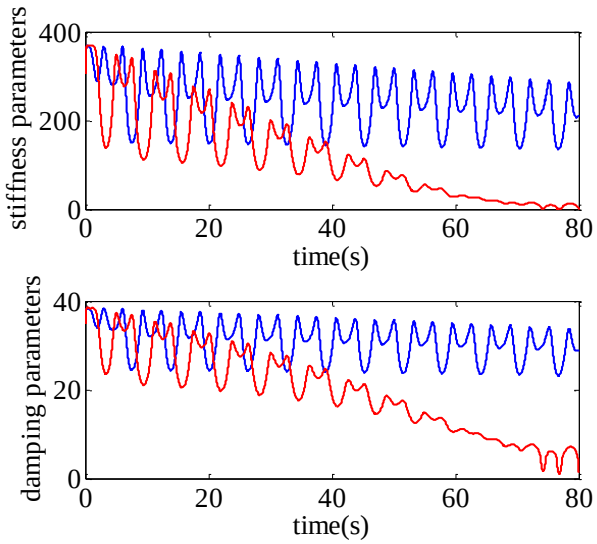


a) Impedance parameters: the first component (blue), and the second component (red).

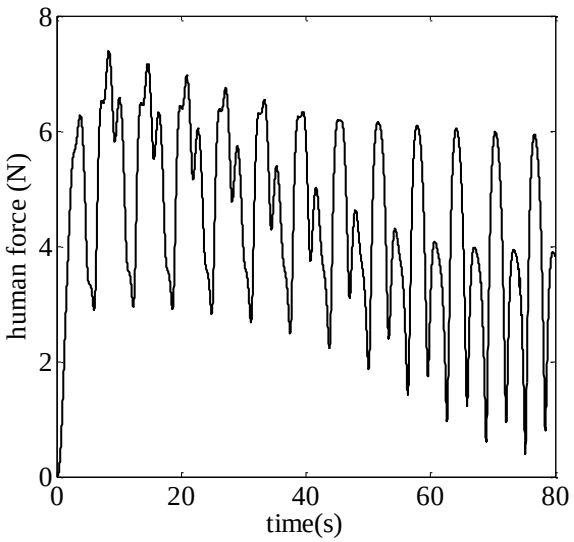


b) Human force in the Cartesian space.

Figure 4. Assistive HRI performance results.

Figure 3 shows the tracking performance of the proposed controller. The ability of the designed controller is shown in Fig. 3 a) - d). Figure 3 a) and b) show the tracking of positions and velocities, respectively. Figure 3 c) shows the desired trajectory, and the actual trajectory of the end-effector in the Cartesian space. As it shows in this figure using the proposed controller, the efficient tracking of the desired trajectory is achieved. Also, as shown in Fig. 3 d) the ultimate boundedness of the model following error signals is achieved by utilizing the proposed control. Figure 3 illustrates that the proposed controller can successfully cope with the tracking problems of the system. The performance of the controller in optimizing the impedance parameters and interaction force is shown in Fig. 4. Figure 4 a) shows the updating of the impedance parameters. Figure 4 b) shows the human-robot interacting force. As shown in Fig. 4, the impedance parameters are tuned such that the

proper assistive human interaction force is achieved. Figures show that using the proposed neural based impedance adaption method, assistive HRI is provided while the stability and boundedness of the closed-loop system is ensured.

In this section, a comparison is performed to show more effectiveness and benefits of the proposed method. To do this, we consider the assistive controller proposed in this paper, and the same controller without the ability of updating the impedance parameters. By that means, we disregard the outer-loop control design and consider the fixed impedance parameters. All the simulation parameters are the same for the first simulation. The simulation results are illustrated in Figs. 5, 6.

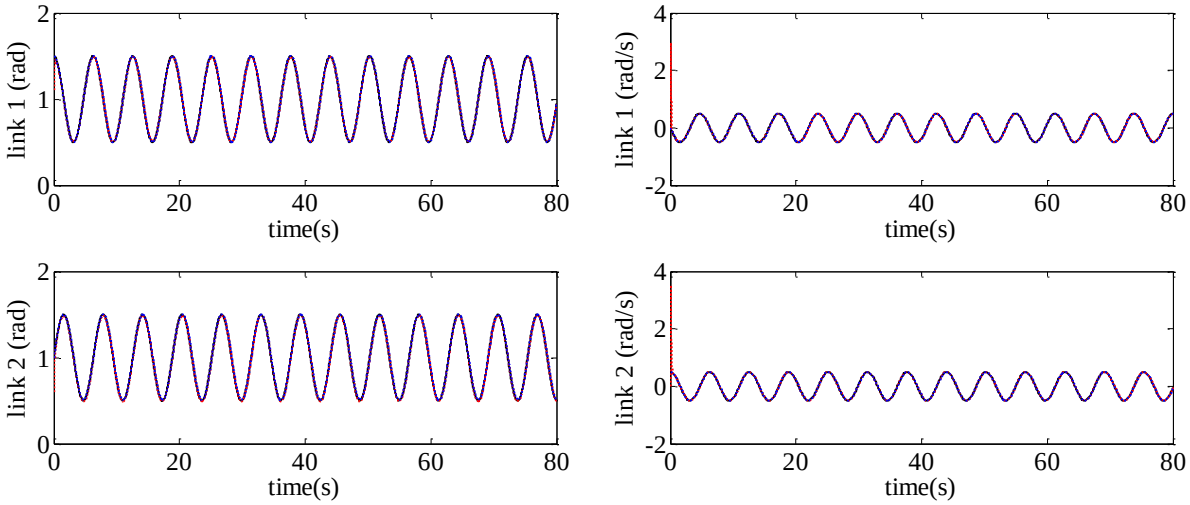


a) The trajectory of positions: the desired signal (black) versus the actual signal (red), and the reference signal (blue).

b) The trajectory of velocities: the desired signal (black) versus the actual signal (red), and the reference signal (blue).

Figure 5. Tracking performance of the system using the fixed impedance control.

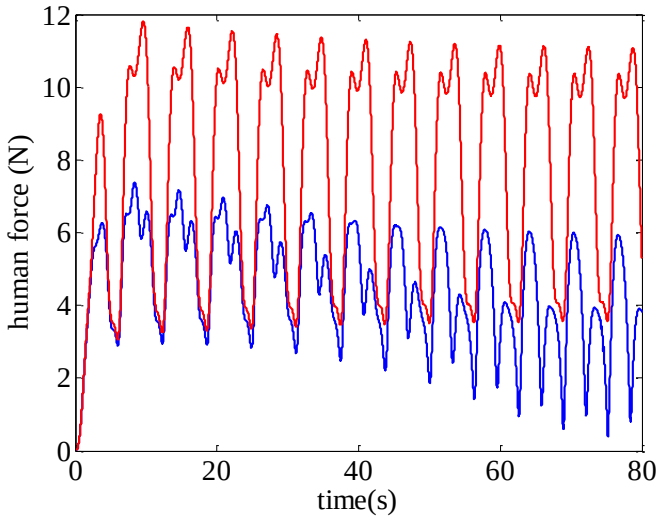


Figure 6. Comparison of the interaction force between the proposed assistive controller (blue), and the fixed impedance control (red).

The tracking performance of the fixed impedance controller is shown in Fig. 5. The figure shows that good tracking is achieved even without updating the impedance parameters. This verifies the ability of the designed neural adaptive impedance inner-loop control in satisfying

a good tracking control performance. The efficiency of the proposed assistive HRI controller in reducing the interaction force is depicted in Fig. 6. This figure shows that using the proposed outer-loop neural network based impedance adaption design, the interaction force is reduced significantly due to its assistive impedance adaption ability. To indicate this effect in a quantified manner, we consider a comparative criterion $\boldsymbol{C}$ as $\boldsymbol{C}=\int_0^{t_f} \boldsymbol{f}_h^2$ and obtain the value of $\boldsymbol{C}$ in both cases. In the fixed impedance case, $\boldsymbol{C}$ is obtained as $\boldsymbol{C}=5477$ while by applying the assistive impedance design, this amount is reduced to $\boldsymbol{C}=1804$. This shows the efficiency of the developed approach to reduce the interaction force, and provide the assistive HRI control.

## 5. Conclusion

A new neuro-adaptive impedance control method has been investigated in this work, to provide assistive HRI. The proposed control scheme has two control loops. First, the inner-loop with the objective of making the unknown robot behave like a prescribed impedance model efficiently while the stability of the system is guaranteed. Second, the outer-loop with the target of developing a framework to assist the human partner to perform a task with the optimized performance. The objective of the inner-loop has been achieved by developing a new adaptive impedance control structure, and utilizing RBF NN to online learn the robot dynamics, and further modifying the obtained control by utilizing the barrier Lyapunov function. The structure of the outer-loop control has been successfully established by developing a backpropagation algorithm to tune the impedance parameters such as to optimize the prescribed cost function. The net result is a stable control structure having intelligent and adaptive characteristics, capable of providing assistive support in HRI while being free from requiring robot dynamics or impedance parameter knowledge.

## 6. References


[1] C.-C. Cheah, D. Wang, Learning impedance control for robotic manipulators, IEEE Transactions on Robotics and Automation, 14 (1998) 452-465.

[2] W.-S. Lu, Q.-H. Meng, Impedance control with adaptation for robotic manipulations, IEEE Transactions on Robotics and Automation, 7 (1991) 408-415.

[3] D. Braun, M. Howard, S. Vijayakumar, Optimal variable stiffness control: formulation and application to explosive movement tasks, Autonomous Robots, 33 (2012) 237-253.

[4] T. Tsumugiwa, R. Yokogawa, K. Hara, Variable impedance control based on estimation of human arm stiffness for human-robot cooperative calligraphic task, IEEE International Conference on Robotics and Automation, (IEEE2002), pp. 644-650.

[5] E. Gribovskaya, A. Kheddar, A. Billard, Motion learning and adaptive impedance for robot control during physical interaction with humans, IEEE International Conference on Robotics and Automation, (IEEE2011), pp. 4326-4332.

[6] C. Wang, Y. Li, S.S. Ge, K.P. Tee, T.H. Lee, Continuous critic learning for robot control in physical human-robot interaction, 13th International Conference on Control, Automation and Systems, (IEEE2013), pp. 833-838.

[7] S. Arimoto, S. Kawamura, F. Miyazaki, Bettering operation of dynamic systems by learning: A new control theory for servomechanism or mechatronics systems, 23rd IEEE Conference on Decision and Control, (IEEE1984), pp. 1064-1069.

[8] S. Arimoto, S. Kawamura, F. Miyazaki, Bettering operation of robots by learning, Journal of Field Robotics, 1 (1984) 123-140.

[9] Y. Li, S.S. Ge, Impedance Learning for Robots Interacting with Unknown Environments, IEEE Transactions on Control Systems Technology, 22 (2014) 1422 - 1432.

[10] H.-S. Ahn, Y. Chen, K.L. Moore, Iterative learning control: Brief survey and categorization, IEEE Transactions on Systems, Man, and Cybernetics, Part C (Applications and Reviews), 37 (2007) 1099-1121.

[11] D.A. Bristow, M. Tharayil, A.G. Alleyne, A survey of iterative learning control, IEEE Control Systems, 26 (2006) 96-114.

[12] D.H. Owens, J. Hätönen, Iterative learning control—An optimization paradigm, Annual reviews in control, 29 (2005) 57-70.
[13] S.S. Ge, Y. Li, C. Wang, Impedance adaptation for optimal robot–environment interaction, International Journal of Control, 87 (2014) 249-263.
[14] R. Ikeura, T. Moriguchi, K. Mizutani, Optimal variable impedance control for a robot and its application to lifting an object with a human, Proceedings of 11th IEEE International Workshop on Robot and Human Interactive Communication (IEEE2002), pp. 500-505.
[15] G. Buizza Avanzini, N.M. Ceriani, A.M. Zanchettin, P. Rocco, L. Bascetta, Safety control of industrial robots based on a distributed distance sensor, IEEE Transactions on Control Systems Technology, 22 (2014) 2127-2140.
[16] S. Oh, H. Woo, K. Kong, Frequency-shaped impedance control for safe human–robot interaction in reference tracking application, IEEE/ASME Transactions On Mechatronics, 19 (2014) 1907-1916.
[17] B. Alqaudi, H. Modares, I. Ranatunga, S.M. Tousif, F.L. Lewis, D.O. Popa, Model reference adaptive impedance control for physical human-robot interaction, Control Theory and Technology, 14 (2016) 68-82.
[18] H. Modares, I. Ranatunga, F.L. Lewis, D.O. Popa, Optimized Assistive Human-Robot Interaction Using Reinforcement Learning, IEEE Transactions on Cybernetics, 46 (2016) 655 - 667.
[19] Y. Li, K.P. Tee, R. Yan, D.K. Limbu, S.S. Ge, Shared control of human and robot by approximate dynamic programming, American Control Conference, (IEEE2015), pp. 1167-1172.
[20] Y. Li, K.P. Tee, W.L. Chan, R. Yan, Y. Chua, D.K. Limbu, Continuous role adaptation for human–robot shared control, IEEE Transactions on Robotics, 31 (2015) 672-681.
[21] Y. Li, K.P. Tee, R. Yan, W.L. Chan, Y. Wu, D.K. Limbu, Adaptive optimal control for coordination in physical human-robot interaction, IEEE/RSJ International Conference on Intelligent Robots and Systems (IROS), (IEEE2015), pp. 20-25.
[22] Y. Li, K.P. Tee, R. Yan, W.L. Chan, Y. Wu, A Framework of Human–Robot Coordination Based on Game Theory and Policy Iteration, IEEE Transactions on Robotics, 32 (2016) 1408-1418.
[23] F.L. Lewis, D.M. Dawson, C.T. Abdallah, Robot manipulator control: theory and practice (CRC Press, 2003).
[24] T.H. Lee, C.J. Harris, Adaptive neural network control of robotic manipulators (World Scientific, 1998).
[25] Y. Li, S.S. Ge, Human–robot collaboration based on motion intention estimation, IEEE/ASME Transactions on Mechatronics, 19 (2014) 1007-1014.
[26] K.P. Tee, E. Burdet, C.-M. Chew, T.E. Milner, A model of force and impedance in human arm movements, Biological cybernetics, 90 (2004) 368-375.
[27] K.P. Tee, D.W. Franklin, M. Kawato, T.E. Milner, E. Burdet, Concurrent adaptation of force and impedance in the redundant muscle system, Biological cybernetics, 102 (2010) 31-44.
[28] H. Yu, T. Xie, S. Paszczynski, B.M. Wilamowski, Advantages of radial basis function networks for dynamic system design, IEEE Transactions on Industrial Electronics, 58 (2011) 5438-5450.
[29] Y. Song, L. Liang, M. Tan, Neuroadaptive Power Tracking Control of Wind Farms Under Uncertain Power Demands, IEEE Transactions on Industrial Electronics, 64 (2017) 7071-7078.
[30] S.S. Ge, C. Wang, Adaptive neural control of uncertain MIMO nonlinear systems, IEEE Transactions on Neural Networks, 15 (2004) 674-692.
[31] K.P. Tee, S.S. Ge, E.H. Tay, Barrier Lyapunov functions for the control of output-constrained nonlinear systems, Automatica, 45 (2009) 918-927.
[32] S.S. Ge, C.C. Hang, T.H. Lee, T. Zhang, Stable adaptive neural network control (Springer Science & Business Media, 2013).
[33] B. Ren, S.S. Ge, K.P. Tee, T.H. Lee, Adaptive neural control for output feedback nonlinear systems using a barrier Lyapunov function, Neural Networks, IEEE Transactions on, 21 (2010) 1339-1345.
[34] M. Sharifi, S. Behzadipour, G. Vossoughi, Nonlinear model reference adaptive impedance control for human–robot interactions, Control Engineering Practice, 32 (2014) 9-27.
[35] C. Wang, Y. Li, S.S. Ge, T.H. Lee, Reference adaptation for robots in physical interactions with unknown environments, IEEE transactions on cybernetics, 47 (2017) 3504-3515.
[36] Y. Song, B. Zhang, K. Zhao, Indirect neuroadaptive control of unknown MIMO systems tracking uncertain target under sensor failures, Automatica, 77 (2017) 103-111.
[37] T.-S. Li, D. Wang, G. Feng, S.-C. Tong, A DSC approach to robust adaptive NN tracking control for strict-feedback nonlinear systems, IEEE Transactions on Systems, Man, and Cybernetics, Part B (Cybernetics), 40 (2010) 915-927.
[38] D. Gorinevsky, On the persistency of excitation in radial basis function network identification of nonlinear systems, IEEE Transactions on Neural Networks, 6 (1995) 1237-1244.